Published OnlineFirst December 6, 2011; DOI: 10.1158/1535-7163.MCT-11-0634

Preclinical Development

Molecular Cancer Therapeutics

Molecular and Cellular Pharmacology of the Hypoxia-Activated Prodrug TH-302

Fanying Meng[1], James W. Evans[1], Deepthi Bhupathi[1], Monica Banica[1], Leslie Lan[1], Gustavo Lorente[1], Jian-Xin Duan[1], Xiaohong Cai[1], Alexandra M. Mowday[2], Christopher P. Guise[2], Andrej Maroz[2], Robert F. Anderson[2], Adam V. Patterson[2], Gregory C. Stachelek[3], Peter M. Glazer[3], Mark D. Matteucci[1], and Charles P. Hart[1]

Abstract

TH-302 is a 2-nitroimidazole triggered hypoxia-activated prodrug (HAP) of bromo-isophosphoramide mustard currently undergoing clinical evaluation. Here, we describe broad-spectrum activity, hypoxia-selective activation, and mechanism of action of TH-302. The concentration and time dependence of TH-302 activation was examined as a function of oxygen concentration, with reference to the prototypic HAP tirapazamine, and showed superior oxygen inhibition of cytotoxicity and much improved dose potency relative to tirapazamine. Enhanced TH-302 cytotoxicity under hypoxia was observed across 32 human cancer cell lines. One-electron reductive enzyme dependence was confirmed using cells overexpressing human NADPH:cytochrome P450 oxidoreductase and radiolytic reduction established the single-electron stoichiometry of TH-302 fragmentation (activation). Examining downstream effects of TH-302 activity, we observed hypoxia-dependent induction of γH2AX phosphorylation, DNA cross-linking, and cell-cycle arrest. We used Chinese hamster ovary cell–based DNA repair mutant cell lines and established that lines deficient in homology-dependent repair, but not lines deficient in base excision, nucleotide excision, or nonhomologous end-joining repair, exhibited marked sensitivity to TH-302 under hypoxia. Consistent with this finding, enhanced sensitivity to TH-302 was also observed in lines deficient in BRCA1, BRCA2, and FANCA. Finally, we characterized TH-302 activity in the three-dimensional tumor spheroid and multicellular layer models. TH-302 showed much enhanced potency in H460 spheroids compared with H460 monolayer cells under normoxia. Multicellular layers composed of mixtures of parental HCT116 cells and HCT116 cells engineered to express an oxygen-insensitive bacterial nitroreductase showed that TH-302 exhibits a significant bystander effect. *Mol Cancer Ther; ©2012 AACR.*

Introduction

Regions of low-oxygen concentration (hypoxia) within solid tumors are a prevalent feature of the cancer phenotype. Both chronic (diffusion-limited) and acute (perfusion-limited) tumor hypoxia have been described and both types of tumor hypoxia arise due to abnormal aspects of tumor vasculature (1). The extent and magnitude of tumor hypoxia has been shown in multiple clinical studies to be a negative prognostic factor (2). Multiple factors underlie the correlation between tumor hypoxia and disease progression; in particular, hypoxic tumor cells resist conventional chemo- and radiation therapies, and hypoxic tumors are more invasive and metastatic. Hypoxia underlies treatment failure for multiple reasons (3): (i) most anticancer therapies target the proliferative aspect of tumor cell growth, and hypoxic cells tend to be quiescent and nonhyperproliferative; (ii) chronic hypoxic regions are relatively inaccessible and require blood-borne chemotherapeutic agents to diffuse long distances to exert their effects; (iii) in the case of radiation therapy resistance, molecular oxygen is a critical requirement for radiation-induced cytotoxicity; (iv) hypoxic cells have lost sensitivity to apoptosis that can lessen the activity of some anticancer agents; and (v) hypoxia upregulates drug resistance proteins. Thus, hypoxic tumor cells are an attractive target for the discovery and development of novel cancer therapies—both because of the central role of tumor hypoxia in treatment resistance and cancer progression—and as hypoxia provides a basis for selective targeting and the sparing of normoxic cells elsewhere in the body. There are a variety of therapeutic strategies being pursued for

Authors' Affiliations: [1]Threshold Pharmaceuticals, South San Francisco, California; [2]Auckland Cancer Society Research Centre, University of Auckland, Auckland, New Zealand; and [3]Department of Therapeutic Radiology, Yale University School of Medicine, New Haven, Connecticut

Note: Supplementary data for this article are available at Molecular Cancer Therapeutics Online (http://mct.aacrjournals.org/).

Corresponding Author: Fanying Meng, Threshold Pharmaceuticals, 170 Harbor Way, Suite 300, South San Francisco, CA 94080. Phone: 650-474-8232; Fax: 650-474-2529; E-mail: fmeng@thresholdpharm.com

doi: 10.1158/1535-7163.MCT-11-0634

©2012 American Association for Cancer Research.

Downloaded from mct.aacrjournals.org on April 29, 2017. © 2011 American Association for Cancer Research.

Published OnlineFirst December 6, 2011; DOI: 10.1158/1535-7163.MCT-11-0634

the selective targeting of hypoxic tumor cells (4). Hypoxia-activated prodrugs (HAP) enable the selective delivery of cytotoxic or cytostatic agents to hypoxic tumor cells. Teicher and Sartorelli first described the use of nitroaromatic-based prodrugs that are selectively activated in hypoxic tumor cells (5). Other synthetic approaches have been described (refs. 6, 7 and reviewed in ref. 8). Select HAPs have progressed to clinical testing and include tirapazamine, AQ4N, PR104, and most recently, TH-302. Tirapazamine has progressed the furthest in clinical testing and has been the subject of late-stage clinical trials (9). No HAP to date has progressed to regulatory approval and clinical use.

An ideal HAP requires the optimization of a number of distinct physical chemical, biochemical, and pharmacologic properties to allow ultimate clinical success as an effective anticancer agent (10). These properties include (i) appropriate tissue diffusion and metabolism/binding properties that are harmonized and thus compatible with deep penetration from the vascular bed into the hypoxic regions of tumors; (ii) the oxygen concentration set-point (*k*-value) for prodrug activation needs to be low enough to minimize activation in normal tissues but high enough to allow activation in regions characteristic of tumor hypoxia; (iii) the released or activated effector should be able to act on both actively dividing and quiescent tumor cells; and (iv) the released effector ideally needs to exhibit moderate reactivity kinetics and an adequate physicochemical profile to allow both cytotoxic action on the activating cells as well as allow some diffusion to adjacent tumor cells to exert a local cytotoxic bystander effect. These select properties are in addition to the typical pharmacokinetic and pharmacodynamic properties that effective drugs require.

We have previously described the synthesis and hypoxia-selective cytotoxicity of TH-302, a 2-nitroimidazole triggered bromo-isophosphoramide mustard (Br-IPM; ref. 11). Here, we describe its *in vitro* pharmacologic profile in detail, including hypoxia-selective cytotoxicity against 32 human cancer cell lines, oxygen dependence of cytotoxicity, drug exposure time, and role of flavoprotein NADPH:cytochrome P450 reductase (POR) expression. The mechanism of action was assessed with γH2AX, DNA cross-linking, cell-cycle analysis, and cell lines defective in specific DNA repair pathways. Finally, multicellular tumor spheroid and multicellular layer (MCL) coculture model systems were used to extend our findings on the ability of TH-302 to penetrate multiple cell layers, selectively activate in hypoxic regions, and exert a local bystander effect.

Materials and Methods

Cell lines

All human cancer cell lines and CHO-K1 and xrs-5 were from the American Type Culture Collection. The POR-overexpressing cells line pairs have been described previously (12). DNA repair mutant Chinese hamster ovary (CHO) cell lines were provided by Martin Brown (Stanford University, Stanford, CA; ref. 13). The UWB1.289 pair was from Elizabeth Swisher (University of Washington, Seattle, WA), the VC-8 pair was from Graeme Smith (KuDOS), and the FANCA pair was from Sara Rockwell (Yale University, New Haven, CT). The cell lines have not been recently tested and reauthenticated.

Reagents and antibodies

Pimonidazole and anti-pimonidazole antibody were from HPI, Inc. The γH2AX mAb and cell-cycle reagents were from Millipore. Fluorescein isothiocyanate (FITC)-conjugated goat antimouse secondary antibody and AlamarBlue were from Invitrogen. Diphenyliodonium chloride (DPI) and puromycin were from Sigma. Bioblend gas mixtures were from Praxair. Comet assay kit was from Trevigen.

Radiation chemistry

Reduction of TH-302 in deaerated solutions was carried using a ^{60}Co γ-ray irradiator calibrated against the Fricke dosimeter. The resulting products were determined using high-performance liquid chromatography/mass spectrometry combined with a diode array/API-ES. Pulse radiolysis studies were conducted as previously described (14).

In vitro cytotoxicity assay

Exponentially growing cells were seeded 24 hours before the addition of test compounds. After drug addition, the plates were incubated for 2 hours, or longer if indicated, under defined oxygen concentrations at 37°C in an anaerobic chamber (Bactron II), a hypoxia chamber (Hypoxystation), or a standard tissue-culture incubator. Using this method, cells equilibrated rapidly (<30 minutes) with the gas phase as shown by linearity of time course of cytotoxicity and use of dissolved oxygen probe (OxyLite, Oxford Optronics). Cells were cultured for 72 hours in complete medium after washing under normoxic conditions, and the viable cells were quantified using AlamarBlue. For DPI experiments, cells were pretreated with 100 μmol/L of DPI for 2 hours under air. Drug concentration resulting in growth inhibition of 50% (IC_{50}) relative to untreated control was calculated using Prism software.

In vitro clonogenic assay

The detailed procedure was described (11). In brief, cells were seeded 24 hours before initiating treatment. Cells were then incubated with the drug for 2 hours under controlled oxygen concentrations. At the end of treatment, cells were plated and placed undisturbed in an incubator for 10 days. Colonies were fixed and stained with crystal violet. Surviving fractions were calculated by dividing the plating efficiencies of treated cells by the plating efficiencies of untreated cells. For VC-8, UWB1.289, and FANCA cell line pairs, cells were plated in triplicate in 6-well plastic plates at 500 to 1,000 cells per well and treated

Downloaded from mct.aacrjournals.org on April 29, 2017. © 2011 American Association for Cancer Research.

Published OnlineFirst December 6, 2011; DOI: 10.1158/1535-7163.MCT-11-0634

with TH-302 for 48 hours under hypoxia and then continuously cultured for approximately 10 days in drug-free media. Cells were stained with crystal violet and colonies of more than 50 cells were counted.

Detection of γH2AX

Cells were treated with vehicle or TH-302 for 2 hours under either normoxic (95% air/5% CO_2) or hypoxic (90% N_2/5% CO_2/5% H_2) conditions and then continuously incubated for the indicated times in the absence of TH-302. H460 cells were permeabilized with 1% Triton X-100 and incubated with γH2AX monoclonal antibody for 2 hours and goat antimouse-FITC for 1 hour. Cells were either imaged using a fluorescent microscope (Nikon T1-SM) or analyzed by flow cytometry (Guava EasyCyte). γH2AX antibody binding were measured using flow cytometry and analyzed using FCS Express software (De Novo Software). The average γH2AX antibody staining relative to untreated controls was calculated on the basis of geometric mean fluorescence.

Comet assay

After seeding cells for 24 hours, TH-302 was added at the indicated concentrations and incubated for 24 hours either under air or 0.1% O_2. Cells were washed twice to remove TH-302 and treated with 20 μmol/L of bleomycin for 1 hour under air. After washing twice with PBS, comet assay was conducted with single-cell electrophoresis system from Trevigen. The data were analyzed using Comet Assay IV software from Perceptive Instruments.

Cell-cycle analysis

Cells were treated with TH-302 for 2 hours under either air or N_2. Following wash, cells were cultured for additional 24 hours. Cells were fixed in 75% ethanol, and cell-cycle distribution was determined using Cell Cycle reagent (Millipore) and flow cytometry (Guava). The cell-cycle data were analyzed using Multicycle analysis software (Phoenix Flow Systems).

Spheroid culture and dissociation

Cells were seeded on 1% agarose-coated plate for 6 hours and then transferred into a T150 flask. Spheroids were continuously cultured and used at either day 8 or day 15. Trypsin was used to dissociate spheroids into a single-cell suspension. For detection of pimonidazole-positive cells, monolayer cells or spheroids were labeled with pimonidazole (100 μmol/L, 2 hours) at the indicated oxygen concentrations. After wash, cells were fixed and stained with FITC anti-pimonidazole antibody (1 hour, room temperature). Pimonidazole-positive cells were detected using flow cytometry and analyzed using FCS Express.

MCL culture bystander assay

The MCL experiments were carried out as previously described (15, 16). The Escherichia coli NfsA–overexpressing HCT116 cell line has been described previously (17). Cell lines were mixed as necessary and seeded into collagen III–coated Millicell-CM membrane inserts (Millipore) and incubated for 3 days at 37°C to form MCLs. Inserts were submerged in media and flushed continuously with 5% CO_2/95% O_2. TH-302 was added to the media for 5 hours and then MCLs were trypsinized, counted, serially diluted, and plated in both nonselective media (α-MEM + 5% FBS) to determine total number of cells and selective media (α-MEM + 5% FBS + 1 μmol/L puromycin) to determine activator cell number. On day 10, colonies containing more than 50 cells were counted. Surviving fractions for each population were calculated as the plating efficiency for drug-treated MCLs/untreated controls. Bystander effect efficiency (BEE) was calculated as

$$\left(\log IC_{90}\ T\text{-}\log IC_{90}T_c\right)/\left(\log IC_{90}T\text{-}\log IC_{90}A_c\right).$$

Results

Radiolytic activation of TH-302

To explore the mechanism of TH-302 activation, pulse and steady-state radiolytic reduction methods were used. Fragmentation occurred under anoxia via the TH-302 radical anion and resulted in elimination of the active cytotoxin Br-IPM (Fig. 1A). Fragmentation was readily inhibited by molecular dioxygen. The measured one-electron reduction potential E(1) and the first-order fragmentation rate constant (k_{frag}) following one-electron reduction were consistent with the proposed mechanism (Fig. 1A, Supplementary Figs. S1–S4). This mechanism is in contrast to the established activation mechanism for 2-nitroimidazoles such as misonidazole and pimonidazole where the radical anion in the absence of oxygen undergoes further reduction to the hydroxyl amine and elimination to a cross-linking nitrenium ion (18, 19).

Oxygen concentration and time dependence of TH-302 activation

To evaluate the stringency of hypoxia required to release the active Br-IPM, we conducted *in vitro* proliferation assay in H460 with different oxygen concentrations. As illustrated in Fig. 1B, TH-302 cytotoxic activity increased as the oxygen level decreased. In addition, hypoxia-selective activation of TH-302 was time-dependent with longer drug exposures providing greater TH-302 potency with a concentration and time relationship that approached linearity (Supplementary Table S1A). A similar profile for HAP tirapazamine was observed although with much lower potency and inferior hypoxia cytotoxicity ratio (HCR) than TH-302 (Fig. 1C and Supplementary Table S1B). This observation was also confirmed with clonogenic assays (Supplementary Fig. S5). In addition, TH-302 requires more severe hypoxia (~0.1% O_2) for high activity, whereas tirapazamine achieves near-maximal activity under conditions of moderate hypoxia (0.6%–1.5% O_2).

Downloaded from mct.aacrjournals.org on April 29, 2017. © 2011 American Association for Cancer Research.

Published OnlineFirst December 6, 2011; DOI: 10.1158/1535-7163.MCT-11-0634

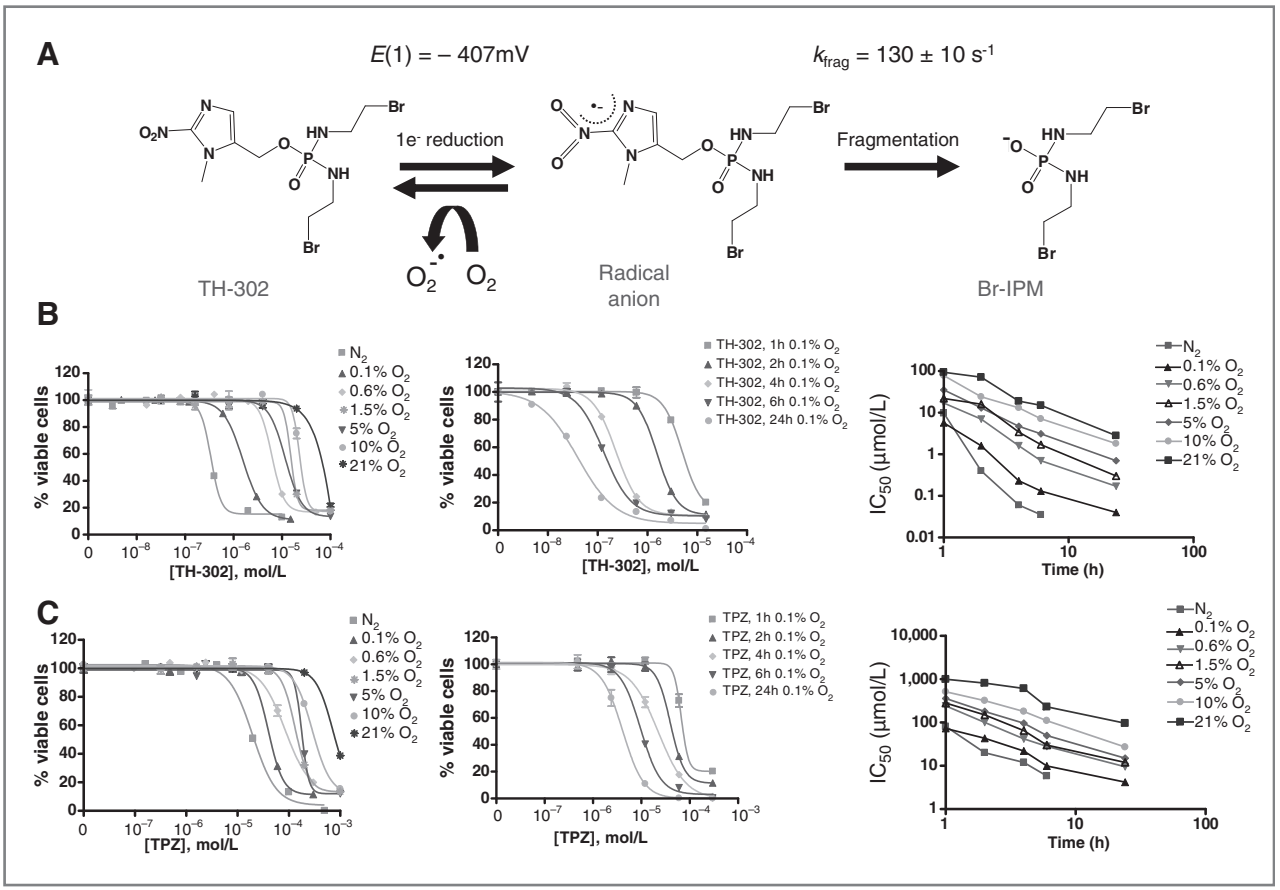

Figure 1. A, schema of TH-302 reductive activation pathway and oxygen concentration- and time-dependent cytotoxicity of TH-302. Direct fragmentation via the radical anion was confirmed by pulse and steady-state reduction. Oxygen concentration- and time-dependent cytotoxicity of TH-302. H460 monolayers were exposed to TH-302 at the indicated oxygen concentrations for 2 hours (B) or 0.1% oxygen for the indicated times in triplicate. Cells were then washed and cultured for up to 72 hours under air in the absence of TH-302. The viable cells were quantified using AlamarBlue and IC_{50s} were calculated using Prism software. IC_{50} summary under different oxygen concentrations as a function of time (Supplementary Table S1A is the mean of 3 independent experiments). H460 monolayers were exposed to tirapazamine at the indicated oxygen concentrations for 2 hours (C) or 0.1% oxygen for the indicated times. Cells were then washed and cultured for up to 72 hours under air in the absence of tirapazamine. The viable cells were quantified using AlamarBlue and IC_{50} values were calculated using Prism software. IC_{50} summary under different oxygen concentrations as a function of time (right; Supplementary Table S1B). TPZ, tirapazamine.

TH-302 exhibits hypoxia-selective cytotoxicity across a panel of human cancer cell lines

TH-302 cytotoxicity was evaluated across 32 human cancer cell lines. As shown in Table 1, TH-302 cytotoxic potency was modest under normoxia with all IC_{50} values greater than 40 μmol/L. In contrast, substantially increased cytotoxicity was observed under hypoxic conditions in all 32 cell lines. Normoxic activity of TH-302 was also examined in the 60 cell line panel of the National Cancer Institute (the NCI-60). IC_{50} values ranged from 1 μmol/L to ≥1,000 μmol/L after 48 hours of continuous drug exposure (Supplementary Table S1C).

Reductase-dependent TH-302 activity

We evaluated the relationship between the potency of TH-302 cytotoxicity and POR expression levels with 2 pairs of matched cell lines (12). As shown in Fig. 2A and Supplementary Table S2, A549 cells overexpressing POR exhibited a 7-fold increase in the potency of TH-302 when tested under hypoxic conditions. A similar magnitude of enhancement of TH-302 potency was also observed under aerobic conditions. TH-302 potency was likewise increased in the SiHa cells overexpressing POR under both hypoxic and aerobic conditions (Fig. 2B and C and Supplementary Table S2). The effect of the mechanism-based flavoenzyme inhibitor DPI (20) on TH-302–mediated cytotoxicity was also examined in SiHa and $SiHa^{POR}$. As shown in Fig. 2B, TH-302 activity under hypoxia can be inhibited by DPI in both SiHa and $SiHa^{POR}$. DPI inhibits TH-302 activity in $SiHa^{POR}$ but not in SiHa under normoxia (Fig. 2C).

TH-302 induces DNA damage

To evaluate whether TH-302 cross-links DNA, we examined the phosphorylation of the histone variant

Downloaded from mct.aacrjournals.org on April 29, 2017. © 2011 American Association for Cancer Research.

Published OnlineFirst December 6, 2011; DOI: 10.1158/1535-7163.MCT-11-0634

Table 1. TH-302 cytotoxicity against a panel of human cancer cell lines after 2 hours of drug exposure under either N_2 or air followed by 3 days incubation under air

Cell line	Cell type	IC_{50} (μmol/L; N_2)	IC_{50} (μmol/L; air)	HCR
H460	Lung	0.1 ± 0.03	55 ± 6	550
H82	Lung	0.3 ± 0.05	40 ± 8	130
Caki-1	Renal	0.4 ± 0.05	56 ± 20	140
ACHN	Renal	0.5 ± 0.3	65 ± 3	130
SK-MEL-5	Melanoma	0.7 ± 0.3	420 ± 120	600
DU145	Prostate	0.7 ± 0.3	170 ± 20	240
HCT116	Colon	0.8 ± 0.2	200 ± 62	250
RPMI-8226	Myeloma	1 ± 0.4	280 ± 27	280
A375	Melanoma	1.1 ± 0.2	190 ± 23	170
PC3	Prostate	1.5 ± 0.4	280 ± 8	190
786-O	Renal	1.7 ± 0.5	200 ± 45	120
MIA PaCa-2	Pancreatic	2.1 ± 0.7	210 ± 49	100
HT1080	Fibrosarcoma	2.4 ± 0.1	>300	>130
SK-MEL-2	Melanoma	5.6 ± 1	730 ± 80	130
MALME-3M	Melanoma	6.3 ± 0.1	330 ± 55	50
KHOS/NP	Osteosarcoma	6.4 ± 2.7	360	60
Calu-6	Lung	6.7 ± 1.6	710 ± 100	110
SiHa	Cervical	6.8 ± 2.2	770 ± 140	110
HT29	Colon	7.8 ± 2.4	>300	>40
BxPC-3	Pancreatic	7.9 ± 0.9	430 ± 85	50
LNCaP	Prostate	8.8 ± 2.3	520 ± 25	60
T47D	Breast	11 ± 4.1	560 ± 57	50
PLC/PRF/5	Hepatoma	11 ± 1	>300	>30
SU.86.86	Pancreatic	11 ± 2.8	470 ± 95	40
SK-BR-3	Breast	12 ± 1.2	360 ± 16	30
Panc-1	Pancreatic	16 ± 4.5	540	30
A549	Lung	20 ± 8.5	610	30
MDA-MB-231	Breast	42 ± 5.7	900 ± 82	20
IGROV-1	Ovary	52 ± 8.5	600 ± 75	12
Hs766T	Pancreatic	60 ± 7.5	1,400	23
SK-MEL-28	Melanoma	60 ± 5.5	>1,000	>16
U87-MG	Glioblastoma-astrocytoma	90 ± 4.5	~1,000	11

NOTE: Results (mean ± SEM) are from 2 or more independent experiments carried out in triplicate.
Abbreviation: HCR, hypoxia cytotoxicity ratio.

H2AX (γH2AX) in H460 cells. There was an increase in γH2AX as a function of time after TH-302 treatment (Supplementary Fig. S6). Under hypoxia, γH2AX signal became readily visible 8 hours after exposure to TH-302 and continued to increase when examined at 24 hours posttreatment. A similar profile was observed for TH-302 under normoxia although a 100-fold higher concentration of TH-302 was required. The TH-302 dose–response for γH2AX induction was also investigated using both flow cytometry and immunofluorescence microscopy. There was an increase in γH2AX as a function of TH-302 concentration. Under hypoxia, TH-302 at 0.13 μmol/L induced visible γH2AX binding after 24 hours posttreatment (Fig. 3B), whereas a greater than 300-fold concentration of TH-302 (45 μmol/L) was required to induce similar γH2AX binding under normoxic conditions (Fig. 3A) and binding intensity was enhanced as TH-302 concentrations increased. A direct biochemical assay for DNA cross-linking, the single-cell electrophoresis-based comet assay, confirmed TH-302–dependent DNA cross-linking (Fig. 3C).

TH-302 causes cell-cycle arrest in a concentration- and hypoxia-dependent manner

H460 cells treated with 0.05 μmol/L of TH-302 under hypoxia led to the accumulation of cells at the G_2–M junction (Fig. 3D and Supplementary Table S3). In contrast, cell-cycle distribution was not altered by 0.05 μmol/L of TH-302 treatment under normoxia (Fig. 3D). As TH-302 concentration was increased, cells arrested at all phases of the cell cycle. A similar profile was observed with HT29 cells (Supplementary Fig. S7 and Table S3).

Downloaded from mct.aacrjournals.org on April 29, 2017. © 2011 American Association for Cancer Research.

Published OnlineFirst December 6, 2011; DOI: 10.1158/1535-7163.MCT-11-0634

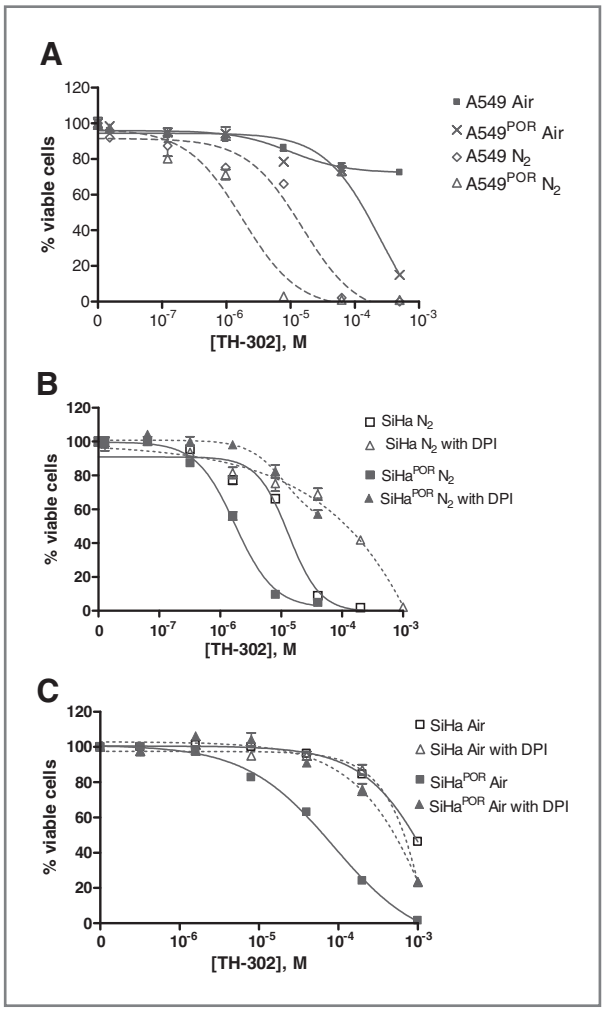

Figure 2. POR-dependent cytotoxicity of TH-302. A549, A549^{POR} (A) and SiHa, SiHa^{POR} (B and C) cell line pairs were treated with TH-302 under either air or N_2 for 2 hours. SiHa and SiHa^{POR} were pretreated with 100 μmol/L of POR inhibitor DPI for 2 hours and then with TH-302 for 2 hours either under N_2 (B) or air (C) in triplicate. After wash, cells were cultured for additional 70 hours under air in the absence of TH-302. The viable cells were quantified using AlamarBlue and IC_{50} values were calculated using Prism software. Similar results were obtained in 2 independent experiments (Supplementary Table S2).

TH-302 enhances cytotoxicity in homology-dependent repair mutant cell lines

To assess the relative importance of different DNA repair pathways involved in TH-302 activity, we first used a panel of CHO cell–based cell lines with defects in different DNA damage response and repair pathways. As shown in Fig. 4A and B and Supplementary Table S4A and S4B, little difference in sensitivity to TH-302 was observed with cells defective in XRCC1 (EM9), ERCC5/XPG (UV135), and Ku80 (xrs-5). These results indicate that base excision repair (BER), nucleotide excision repair (NER), and nonhomologous end-joining (NHEJ), respectively, are not significantly involved in the response and repair of TH-302 adducts. However, irs1SF cells (defective in XRCC3) showed either a 7-fold increase (Fig. 4A and Supplementary Table S4A) or 33-fold increase (Fig. 4C and Supplementary Table S4C) in sensitivity to TH-302. UV41 cells (defective in ERCC4/XPF) exhibited a 67-fold increase in TH-302 sensitivity (Fig. 4A). Cell line pairs composed of one line deficient in BRCA1, BRCA2, or FANCA and a matched line complemented by the overexpression of the corresponding wild-type proteins were also tested for their relative sensitivity to TH-302. As shown in Fig. 4D–F and Supplementary Table S4D, all 3 of the deficient lines exhibited an enhanced sensitivity to TH-302 compared with the wild-type protein complemented cognate lines. The *BRCA2* mutant line was particularly sensitive, exhibiting a subnanomolar IC_{90} (0.6 nmol/L) for TH-302 when tested under hypoxic conditions. Taken together, the results indicate that homology-dependent repair (HDR) pathways are those primarily involved in TH-302 DNA damage repair.

Monoalkylating TH-302 analogue activity

To investigate the importance of bisfunctionality and cross-linking for TH-302 activity, we compared the potency of TH-302 with TH-1197, an analogue with only one reactive bromine leaving group (Supplementary Fig. S8). TH-302 exhibited 33-fold greater activity in AA8 wild-type cells under anoxia (IC_{50} = 2.6 μmol/L) than in TH-1197 (IC_{50} = 87 μmol/L). In HDR-defective cells (irs1SF), an even greater enhancement (180-fold) of TH-302 potency (IC_{50} = 0.14 μmol/L) was observed than that of TH-1197 (IC_{50} = 25 μmol/L) under anoxia.

TH-302 activity in 3-dimensional multicellular tumor spheroid model

Human tumor spheroids recapitulate aspects of the tumor microenvironment, including multiple cell layers for drug penetration and oxygen concentration gradients. As shown in Fig. 5A, 79% of H460 spheroid cells were pimonidazole-positive when incubated under 21% O_2 conditions indicative of significant diffusion limited hypoxia. TH-302 showed 650-fold greater activity in H460 spheroids than in monolayer cells with IC_{50} values of 0.1 and 65 μmol/L, respectively (Fig. 5B and Supplementary Table S5A). In contrast, tirapazamine exhibited only a 4-fold difference between monolayer and spheroids, which is consistent with previous studies (21). This observation was confirmed using clonogenic assays with day 15 spheroids (Supplementary Fig. S9A) and day 8 spheroids (Supplementary Fig. S9B). The anthracycline chemotherapeutic daunorubicin exhibited the converse pattern of greater potency against monolayer cells, which was expected given its poor tissue penetration properties. The results are consistent with TH-302 exhibiting good penetrability, hypoxia activation, and bystander effect.

Enhanced activity of TH-302 in spheroids is due to microenvironmental factors

To determine the basis for the TH-302 sensitivity difference between monolayer cells and cells from spheroids,

Downloaded from mct.aacrjournals.org on April 29, 2017. © 2011 American Association for Cancer Research.

Published OnlineFirst December 6, 2011; DOI: 10.1158/1535-7163.MCT-11-0634

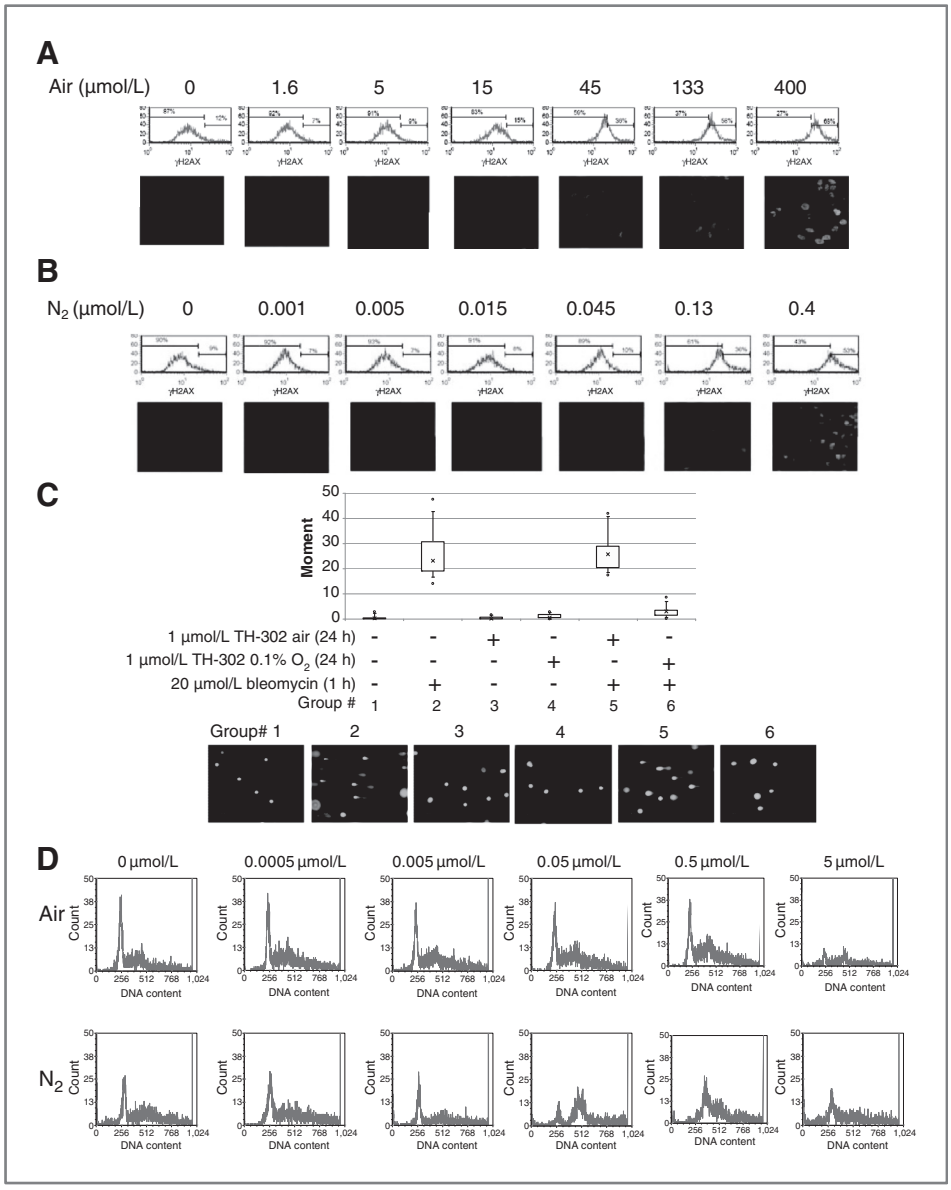

Figure 3. TH-302–mediated concentration-dependent induction of γH2AX, DNA cross-linking, and cell-cycle arrest. H460 cells were treated with TH-302 either under air (A) or under N_2 (B) for 2 hours at the indicated concentrations, and then washed to remove TH-302. Cells were continuously cultured in TH-302–free medium for additional 22 hours. Cells were then harvested and fixed. γH2AX binding was detected using either flow cytometry or fluorescence microscopy. Similar results were obtained in 2 independent experiments. TH-302–mediated DNA cross-linking was investigated using the comet assay. Cells were treated with TH-302 for 24 hours and then exposed to bleomycin for 1 hour. Tails were visualized using fluorescent microscope, and the tail moment box chart (C) was generated using Comet IV software and the TH-302–mediated cell G_2–M, and pan-cycle arrest was characterized using flow cytometry in H460 cells (D and Supplementary Table S3) and in HT29 cells (Supplementary Fig. S7).

we compared the cytotoxic activity of TH-302 between intact spheroids, suspended cells from dissociated spheroids cells, monolayer cultures, and suspended cells from monolayer cultures. Consistent with the proposed mechanism of activation, enhanced sensitivity to TH-302 is only observed in intact H460 spheroids (IC_{50} = 0.2 μmol/L) and not in cells from dissociated spheroids (IC_{50} = 21 μmol/L; Fig. 5C and Supplementary Table S5B). Cell sensitivity to TH-302 was not altered by trypsinization. Hypoxic cell population was only detected in intact spheroids but not in suspended cells from dissociated spheroids cells (Supplementary Fig. S9C). Taken together, the results indicate that the dramatic TH-302 potency shift in spheroids is due largely to the spheroid microenvironment and is not a consequence of cell autonomous changes dependent on spheroid-based cell propagation.

Demonstration of bystander effect with MCL cultures

To confirm the ability of TH-302 to exhibit a bystander effect, where warhead released in hypoxic cells is able to diffuse locally to kill adjacent cells, we used a mixture of TH-302–sensitive and -resistant cell populations grown as 3-dimensional cocultures (15, 16). As shown in Fig. 5D and Supplementary Table S5C, parental HCT116 cells (target cells) were relatively resistant to TH-302 exposure under hyperoxic (95% O_2) conditions with IC_{90} of 19 μmol/L. Hyperoxic conditions serve to suppress the endogenous $1e^-$ reductase–mediated prodrug activation by enhancing the O_2 concentration–mediated back-reaction from radical anion to prodrug (Fig. 1A). HCT116 cells engineered to express the 2-electron nitroreductase NfsA (activator cells) displayed a marked sensitivity to TH-302 exposure

Downloaded from mct.aacrjournals.org on April 29, 2017. © 2011 American Association for Cancer Research.

Published OnlineFirst December 6, 2011; DOI: 10.1158/1535-7163.MCT-11-0634

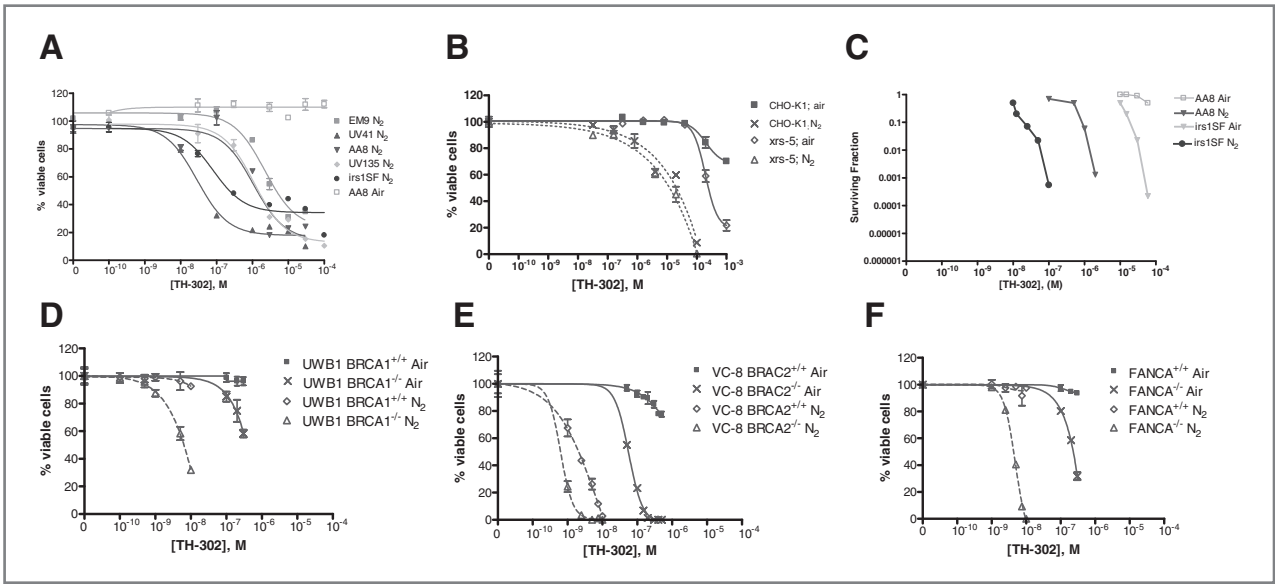

Figure 4. Enhanced TH-302 sensitivity in HDR-defective cell lines. A, wild-type CHO-based parental AA8 cells and isogenic DNA repair mutant cell lines, EM9, UV41, UV135, and irs1SF. Wild-type CHO-K1 and isogenic DNA repair mutant line xrs-5 (B); AA8 and irs1SF (C); BRCA1 wild-type and mutant (D); BRCA2 wild-type and mutant (E); and FANCA wild-type and mutant (F) were treated with TH-302 in triplicate under either hypoxic or normoxic conditions. Dose-dependent *in vitro* cytotoxicity by proliferation-based assays (A and B) or clonogenic-based assay (C–F) were quantified (Supplementary Table S4A–S4D). Similar results were obtained in at least 2 independent experiments.

under hyperoxia with IC_{90} value of 0.09 μmol/L. While target cells alone were refractory, when grown in coculture with 30% activators, they experienced a marked 10-fold reduction in surviving fraction (IC_{90}). The calculated BEE was 43% indicating that the active metabolites generated by TH-302 reduction are able to diffuse out of the cell of origin and act on surrounding neighboring target cells.

Discussion

The selective targeting of the hypoxic compartment of tumors provides an approach for the development of novel anticancer therapies. HAPs, based on oxygen concentration–sensitive nitroheterocyclic bioreductive triggers linked to cytotoxic or cytostatic effectors, are an especially attractive design (10).

We established the one-electron reduction stoichiometry of TH-302 to fragment via the radical anion and release the cytotoxic warhead Br-IPM. The rate of fragmentation ($k_{frag} = 130 \pm 10\ s^{-1}$) is first-order and sufficiently slow to be readily inhibited (back-oxidized) by molecular dioxygen (14).

Having confirmed the oxygen-sensitive free radical–dependent mechanism of TH-302 activation, we next used multiple oxygen concentrations to profile TH-302 and compare its relative oxygen concentration potency with the prototypical HAP tirapazamine (22, 23). Different lengths of time for drug exposure under the oxygen concentration atmospheres were used. We observed that tirapazamine achieved near-maximal activity against H460 cells under conditions of moderate hypoxia (~1.5%–0.6% O_2), which is consistent with the reported oxygen concentration required for half-maximal cytotoxicity in V79 (22) and SiHa cells (23). Conversely, for TH-302, most of its selectivity (~375-fold) is only obtained at 0.1% or less, with 0.6% O_2 providing only moderate potency compared with 21%. This result is consistent with targeting the more severe pathologic hypoxia associated with tumor subregions while sparing moderate hypoxic regions found in certain normal tissues.

We then tested the hypoxia-selective cytotoxicity profile of TH-302 across 32 human cancer cell lines. All cell lines examined exhibited enhanced cytotoxicity when the TH-302 exposure was conducted under hypoxic conditions. Of particular note was the finding of a wide range of potencies that spanned more than 2 orders of magnitude among the individual cell lines examined.

Given the variety of different mechanisms underlying the activation and mechanism of action of TH-302, there are a number of differences between the cells, which either alone or in combination could underlie the wide variation in potency observed. These factors could include differences in the activity of one-electron reductases, differences in DNA repair mechanisms, and differences in cell fate (cell-cycle arrest, cell death) as a function of DNA damage. Overall, aerobic potency was low and cytotoxicity was enhanced under hypoxic conditions. This result can be contrasted to other HAPs that exhibit both hypoxia-dependent and hypoxia-independent activation. For example, in addition to being activated by 1-electron reductases in a hypoxia-dependent manner, the HAP PR104A is also activated in a hypoxia-independent manner by the 2-electron oxidoreductase aldo-keto reductase 1C3 (24). Cell lines in which this reductase is highly

Downloaded from mct.aacrjournals.org on April 29, 2017. © 2011 American Association for Cancer Research.

Published OnlineFirst December 6, 2011; DOI: 10.1158/1535-7163.MCT-11-0634

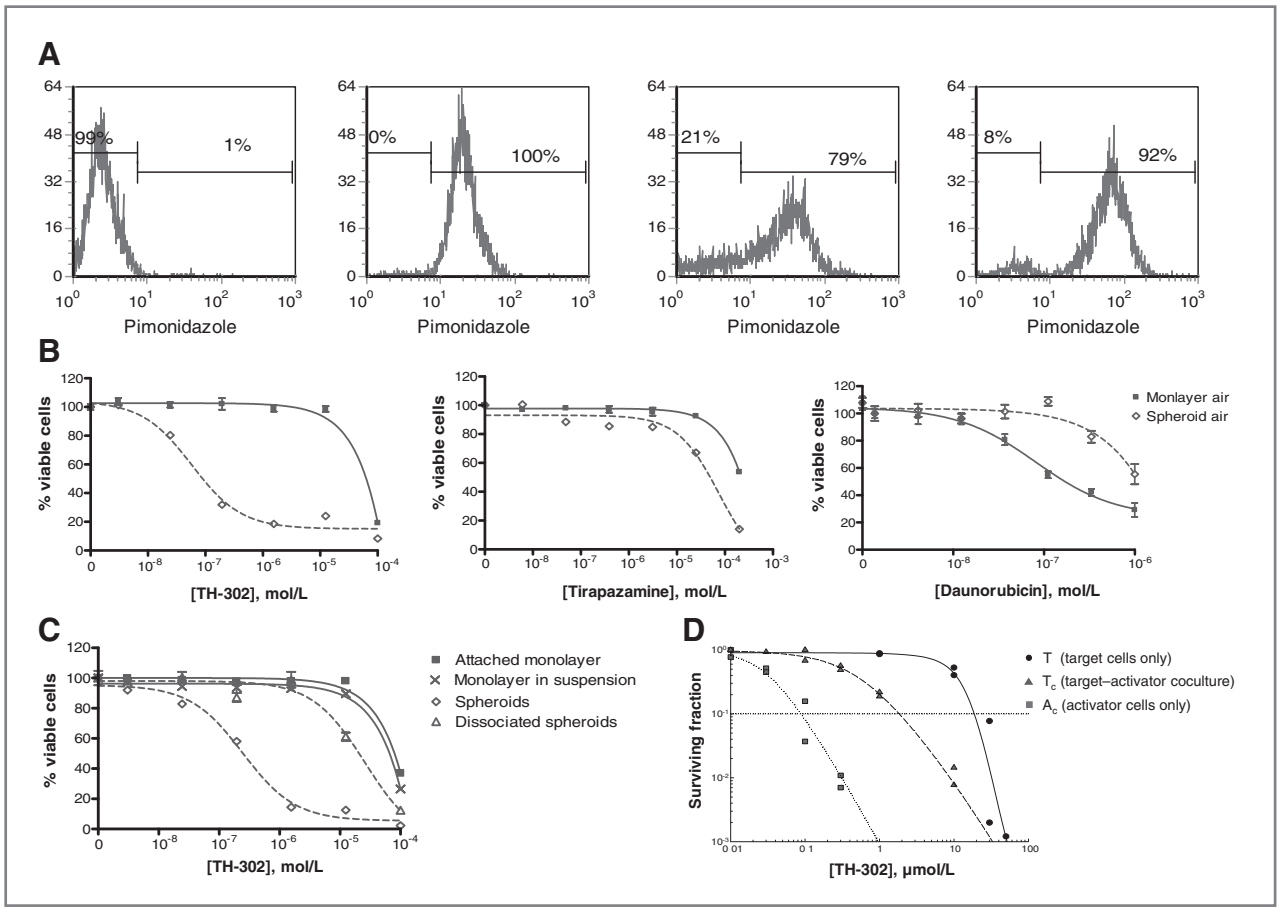

Figure 5. Enhanced TH-302 activity in H460 spheroids compared with H460 monolayers and demonstration of bystander effect with MCLs. Hypoxic population (A) in monolayers under air, monolayers under hypoxia, spheroids under air, and spheroids under hypoxia was determined by pimonidazole staining and flow cytometry. H460 spheroids and monolayers were treated with TH-302, tirapazamine, or daunorubicin at various concentrations for 2 hours using either monolayer cells (solid line) or spheroids (dashed line), and cytotoxicity was assessed using AlamarBlue (B). TH-302 activity was also examined in H460 monolayers, H460 single-cell suspensions derived from monolayers, H460 spheroids, and single-cell suspensions derived from spheroids (C). Similar results were obtained in 3 independent experiments (Supplementary Table S5A and S5B). TH-302 dose–response curves for hyperoxic (5 hours, 95% O_2) MCLs of HCT116 parental target cells in the absence (T) and presence (T_c) of NfsA nitroreductase-expressing HCT116 activator cells (D). MCLs are composed of targets only (T) or as coculture mixtures of 29% ($\pm$ 4%) activators (A) and 71% targets (T_c). Displacement of the target cell survival curve to the left (T to T_c) is indicative of the presence of a cytotoxic metabolite(s) able to diffuse out of the sensitive activator (D) cell population. The calculated BEE was 43.4%. Results were obtained from 2 independent experiments (Supplementary Table S5C).

expressed exhibit sensitivity to PR-104A in a hypoxia-independent manner (25). Currently, no evidence exists to support a similar pathway of aerobic activation for TH-302 despite extensive cell line studies.

The 2-nitroimidazole system has been partially characterized with regard to the spectrum of enzymes capable of catalyzing this initial reduction (26) although uncertainties still remain (27). Walton and Workman first showed the role of POR in the reduction of 2-nitroimidazole (26). Patterson and colleagues (28) showed a correlation of POR activity levels with the magnitude of HAP activation and cytotoxicity. We tested the ability of POR to serve as an activating enzyme for TH-302. We observed a marked increase of potency of TH-302 in the lines overexpressing POR. The enhanced activity can be inhibited by the pan-flavoenzyme inhibitor DPI. These results are consistent with the differential expression and activity of POR potentially serving as one factor underlying the wide range of potencies observed for TH-302 among different human cancer cell lines. These results also support the hypothesis that the relative reductase levels in both tumor and normal tissue may contribute to the magnitude of the clinical benefit and the therapeutic index in patients. Advances in biomarker analysis of individual patients, whether based on tissue biopsies, serum or plasma samples, or circulating tumor cells, could be applied to patients and help guide decisions on TH-302 treatment based on POR or other activating enzymes identified. Population-level analysis of POR expression suggests a high frequency of expression in malignancies of the ovary and liver (29).

We used a series of assays to explore the mechanism of action of TH-302. Given the bis-alkylator nature of the warhead, our efforts were focused on DNA damage pathways. Histone H2AX phosphorylation (γH2AX) has

Downloaded from mct.aacrjournals.org on April 29, 2017. © 2011 American Association for Cancer Research.

Published OnlineFirst December 6, 2011; DOI: 10.1158/1535-7163.MCT-11-0634

emerged as a robust and sensitive marker of the action of DNA interstrand cross-linking (ICL) agents (30, 31). We show here both a TH-302 concentration- and time-dependent induction of γH2AX by both immunohistochemistry and flow cytometric techniques. The concentrations of TH-302 necessary to induce γH2AX were of the same magnitude as those required for cell death and the observed time course was similar to that described previously for other DNA cross-linking agents. Comet assay profiling (32) confirmed TH-302–induced DNA cross-linking. The observed cell-cycle effects are consistent with the DNA-targeted mechanism of action for TH-302. Similar cell-cycle effects have been described in multiple myeloma cell lines treated with TH-302 (33).

To explore the specific nature of the DNA lesions that induced the γH2AX signaling and subsequent cytotoxicity, we used a panel of matched cell line pairs that are defective in distinct DNA damage repair enzymes (34–36). The specific pathways we profiled included NER, BER, NHEJ, and HDR, and mutants deficient in HDR proteins (37, 38) exhibited greatly enhanced sensitivity to TH-302. BRCA and Fanconi proteins also play key roles in the response of cells to DNA damage that results in HDR-based repair (39, 40). Using paired cell lines defective in BRCA1, BRCA2, or FANCA together with their wild-type protein expressing isogenic controls, TH-302 exhibited an enhanced cytotoxic potency in the mutant lines. Taken together, these results clearly implicate HDR as the pathway primarily responsible for the repair of TH-302–induced DNA damage. This HDR pathway has also been shown to be a principal pathway for the repair of DNA damage induced by the HAPs tirapazamine (13) and PR104A (41). Interestingly, using one of the same pairs of lines (AA8 and irs1SF), Evans and colleagues observed a 4× enhanced potency of tirapazamine in the irs1SF compared with the wild-type whereas we observed a 50× enhancement with TH-302. This difference is consistent with the activity of TH-302 being more specific to the HDR mechanism of action as tirapazamine was shown to also yield lesion repair by BER (13). The findings that TH-302 activity is enhanced in the context of HDR repair pathways is of particular note because of the recent finding that hypoxia results in decreased expression of homologous recombination proteins, including XRCC-3, (the protein mutated in the irs1SF line), BRCA1, as well as other HDR-related genes (42–44). This observation indicates that the *in vivo* sensitivity to TH-302–mediated DNA damage may be enhanced in the same hypoxic compartment of the tumor where the prodrug activation occurs. This could contribute to a favorable therapeutic index if the cells responsible for prodrug activation are inherently more sensitive to the released warhead than non-hypoxic cells. In addition, these mechanisms of action results have implications for the clinical use of TH-302. Patient tumors with deficiencies in HDR (e.g., through XRCC, FANC, or BRCA mutations or other HDR defects) would be expected to be hypersensitive to TH-302. These results provide the basis for the development of diagnostic tests that could identify patients most likely to benefit from TH-302 based on their HDR status. For example, the potential prognostic value of the *BRCA*-like profile in ovarian carcinomas (45) may be of interest, particularly if associated with the observations of elevated POR expression (29). Likewise, cancer drugs that that have been shown to downregulate HDR, such as the approved agents gemcitabine, vorinostat, bortezomib, and imatinib (46–49), may combine with TH-302 in additive or synergistic manners due to complementary mechanisms of action.

Three-dimensional multicellular tumor spheroids recapitulate many aspects of the tumor microenvironment and are an especially relevant *in vitro* model system to profile the multiparametric pharmacologic activities of HAPs. Here, we show that TH-302 kills a very high fraction of spheroid cells, especially in comparison with the benchmark HAP tirapazamine. Essentially, all of the increase in TH-302 potency observed in the spheroid model can be ascribed to the microenvironment of the spheroid system.

MCLs composed of mixtures of two metabolically distinct cell populations are a useful method for assessing HAP bystander effect potential. The approach uses one cell type that can efficiently activate TH-302 and is subject to its cytotoxic effects and a second cell type that cannot activate TH-302 but may be subject to the cytotoxic effect of the diffusible cytotoxin if it is released from activator cells (15, 16). By using a two-electron bacterial nitroreductase under hyperoxic conditions, clean metabolic boundaries are created at the cellular level, a model that is difficult to reproduce using oxygen gradients (15, 17). The TH-302 IC_{90} values for the two cell types were 19 and 0.09 μmol/L, respectively. This ∼200× ratio is broadly aligned with cytotoxicity ratios observed with human cancer cell lines when profiled under oxic and hypoxic conditions. The proportion of activator cells in the MCLs ranged from 25% to 33%. This proportion of metabolically active hypoxic cells is typical of human tumour xenografts as measured by pimonidazole binding. Thus, the magnitude of the sensitizing effect and the quantum of metabolically active cells in the MCL were considered broadly analogous to the hypoxic cell compartment found in xenograft models. When the resistant target cells were cocultured with this minority population activator cells under hyperoxic conditions (95% O_2/5% CO_2) that suppresses endogenous one-electron reductase–mediated prodrug activation, TH-302 cytotoxicity was acquired via a process of cell-to-cell released warhead transfer. The calculated BEE was 43%, which is indicative of a bystander effect of intermediate efficiency. The TH-302 bystander effect can be compared with HAPs exhibiting a large bystander effect, for example, the 3,5-dinitrobenzamine-2-bromomustard SN27686, with BEE values more than 90% (16), and HAPs with no bystander effect, for example, tirapazamine, with BEE values estimated at 0% (15). The intermediate nature of the bystander effect of TH-302 provides theoretical advantages whereby active metabolite concentrations are not excessively diluted as a

Downloaded from mct.aacrjournals.org on April 29, 2017. © 2011 American Association for Cancer Research.

Published OnlineFirst December 6, 2011; DOI: 10.1158/1535-7163.MCT-11-0634

function of long-range diffusion distances but rather provide a localized effect against adjacent cells at intermediate oxygen tensions considered to be a critically important subpopulation (50). An intermediate diffusion range also has the added advantage that the probability of systemic recirculation of activated warhead is minimized.

In conclusion, the results described here highlight TH-302 as an optimized HAP. The wide range of human tumor cell lines in which it exhibits hypoxia-selective cytotoxicity, coupled with no evidence consistent with hypoxia-independent mechanism of cytotoxicity, supports the potential for its broad applicability in the context of established chemotherapy and radiotherapy regimens. The described oxygen concentration profile for activation is consistent with the selective targeting of the deep hypoxia found in solid tumors and minor activation in tissues exhibiting nonpathologic moderate hypoxia. The dependence of cytotoxicity on POR expression highlights the potential to profile the expression of this and other one-electron oxidoreductases. Identification of the pathways of DNA damage response and repair involved with the activity of TH-302 point to mechanisms of sensitivity or resistance that could have relevance to the clinical use of TH-302. TH-302 is currently in clinical trials for the treatment of cancer.

Disclosure of Potential Conflicts of Interest

F. Meng, J.W. Evans, D. Bhupathi, M. Banica, L. Lan, G. Lorente, J.-X. Duan, X. Cai, M.D. Matteucci, and C.P. Hart are current or former employees and stockholders of Threshold Pharmaceuticals, Inc.

Grant Support

This study was funded in part by Health Research Council of New Zealand grants 08/103 (A.V. Patterson, C.P. Guise, A.M. Mowday), 09/124 (R.F. Anderson, A. Maroz), and NIH grant P01 CA129186 (P.M. Glazer).

The costs of publication of this article were defrayed in part by the payment of page charges. This article must therefore be hereby marked *advertisement* in accordance with 18 U.S.C. Section 1734 solely to indicate this fact.

Received August 17, 2011; revised November 18, 2011; accepted November 22, 2011; published OnlineFirst December 6, 2011.

References

1. Hockel M, Vaupel P. Tumor hypoxia: definitions and current clinical, biologic, and molecular aspects. J Natl Cancer Inst 2001;93:266–76.
2. Vaupel P, Mayer A. Hypoxia in cancer: significance and impact on clinical outcome. Cancer Metastasis Rev 2007;26:225–39.
3. Wilson WR, Hay MP. Targeting hypoxia in cancer therapy. Nat Rev Cancer 2011;11:393–410.
4. Brown JM, Wilson WR. Exploiting tumour hypoxia in cancer treatment. Nat Rev Cancer 2004;4:437–47.
5. Teicher BA, Sartorelli AC. Nitrobenzyl halides and carbamates as prototype bioreductive alkylating agents. J Med Chem 1980;23:955–60.
6. Denny WA, Wilson WR. Considerations for the design of nitrophenyl mustards as agents with selective toxicity for hypoxic tumor cells. J Med Chem 1986;29:879–87.
7. Firestone A, Mulcahy RT, Borch RF. Nitroheterocycle reduction as a paradigm for intramolecular catalysis of drug delivery to hypoxic cells. J Med Chem 1991;34:2933–5.
8. Chen Y, Hu L. Design of anticancer prodrugs for reductive activation. Med Res Rev 2009;29:29–64.
9. Reddy SB, Williamson SK. Tirapazamine: a novel agent targeting hypoxic tumor cells. Expert Opin Investig Drugs 2009;18:77–87.
10. Denny WA, Wilson WR. Bioreducible mustards: a paradigm for hypoxia-selective prodrugs of diffusible cytotoxins (HPDCs). Cancer Metastasis Rev 1993;12:135–51.
11. Duan JX, Jiao H, Kaizerman J, Stanton T, Evans JW, Lan L, et al. Potent and highly selective hypoxia-activated achiral phosphoramidate mustards as anticancer drugs. J Med Chem 2008;51:2412–20.
12. Guise CP, Wang AT, Theil A, Bridewell DJ, Wilson WR, Patterson AV. Identification of human reductases that activate the dinitrobenzamide mustard prodrug PR-104A: a role for NADPH:cytochrome P450 oxidoreductase under hypoxia. Biochem Pharmacol 2007;74:810–20.
13. Evans JW, Chernikova SB, Kachnic LA, Banath JP, Sordet O, Delahoussaye YM, et al. Homologous recombination is the principal pathway for the repair of DNA damage induced by tirapazamine in mammalian cells. Cancer Res 2008;68:257–65.
14. Anderson RF, Denny WA, Li W, Packer JE, Tercel M, Wilson WR. Pulse radiolysis studies on the fragmentation of arylmethyl quaternary nitrogen mustards by one-electron reduction in aqueous solution. J Phys Chem A 1997;101:9704–9.
15. Wilson WR, Hicks KO, Pullen SM, Ferry DM, Helsby NA, Patterson AV. Bystander effects of bioreductive drugs: potential for exploiting pathological tumor hypoxia with dinitrobenzamide mustards. Radiat Res 2007;167:625–36.
16. Singleton DC, Li D, Bai SY, Syddall SP, Smaill JB, Shen Y, et al. The nitroreductase prodrug SN 28343 enhances the potency of systemically administered armed oncolytic adenovirus ONYX-411(NTR). Cancer Gene Ther 2007;14:953–67.
17. Prosser GA, Copp JN, Syddall SP, Williams EM, Smaill JB, Wilson WR, et al. Discovery and evaluation of Escherichia coli nitroreductases that activate the anti-cancer prodrug CB1954. Biochem Pharmacol 2010;79:678–87.
18. Wardman P, Dennis MF, Everett SA, Patel KB, Stratford MR, Tracy M. Radicals from one-electron reduction of nitro compounds, aromatic N-oxides and quinones: the kinetic basis for hypoxia-selective, bioreductive drugs. Biochem Soc Symp 1995;61:171–94.
19. Bolton JL, McClelland RA. Kinetics and mechanism of the decomposition in aqueous solutions of 2-(Hydroxyamino)imidazoles. J Am Chem Soc 1989;111:8172–81.
20. Tew DG. Inhibition of cytochrome P450 reductase by the diphenyliodonium cation. Kinetic analysis and covalent modifications. Biochemistry 1993;32:10209–15.
21. Durand RE, Olive PL. Evaluation of bioreductive drugs in multicell spheroids. Int J Radiat Oncol Biol Phys 1992;22:689–92.
22. Koch CJ. Unusual oxygen concentration dependence of toxicity of SR-4233, a hypoxic cell toxin. Cancer Res 1993;53:3992–7.
23. Hicks KO, Siim BG, Pruijn FB, Wilson WR. Oxygen dependence of the metabolic activation and cytotoxicity of tirapazamine: implications for extravascular transport and activity in tumors. Radiat Res 2004;161:656–66.
24. Guise CP, Abbattista MR, Singleton RS, Holford SD, Connolly J, Dachs GU, et al. The bioreductive prodrug PR-104A is activated under aerobic conditions by human aldo-keto reductase 1C3. Cancer Res 2010;70:1573–84.
25. Singleton RS, Guise CP, Ferry DM, Pullen SM, Dorie MJ, Brown JM, et al. DNA cross-links in human tumor cells exposed to the prodrug PR-104A: relationships to hypoxia, bioreductive metabolism, and cytotoxicity. Cancer Res 2009;69:3884–91.
26. Walton MI, Workman P. Nitroimidazole bioreductive metabolism. Quantitation and characterisation of mouse tissue benznidazole nitroreductases *in vivo* and *in vitro*. Biochem Pharmacol 1987;36:887–96.
27. Joseph P, Jaiswal AK, Stobbe CC, Chapman JD. The role of specific reductases in the intracellular activation and binding of 2-nitroimidazoles. Int J Radiat Oncol Biol Phys 1994;29:351–5.

Downloaded from mct.aacrjournals.org on April 29, 2017. © 2011 American Association for Cancer Research.

Published OnlineFirst December 6, 2011; DOI: 10.1158/1535-7163.MCT-11-0634

28. Patterson AV, Saunders MP, Chinje EC, Talbot DC, Harris AL, Strafford IJ. Overexpression of human NADPH:cytochrome c (P450) reductase confers enhanced sensitivity to both tirapazamine (SR 4233) and RSU 1069. Br J Cancer 1997;76:1338–47.
29. Guise CP, Abbattista MR, Tipparaju SR, Lambie NK, Su J, Li D, et al. Diflavin oxidoreductases activate the bioreductive prodrug PR104A under hypoxia. Mol Pharmacol 2012;81:1–10.
30. Olive PL, Banath JP. Kinetics of H2AX phosphorylation after exposure to cisplatin. Cytometry B Clin Cytom 2009;76:79–90.
31. Clingen PH, Wu JY, Miller J, Mistry N, Chin F, Wynne P, et al. Histone H2AX phosphorylation as a molecular pharmacological marker for DNA interstrand crosslink cancer chemotherapy. Biochem Pharmacol 2008;76:19–27.
32. Ostling O, Johanson KJ. Microelectrophoretic study of radiation-induced DNA damages in individual mammalian cells. Biochem Biophys Res Commun 1984;123:291–8.
33. Hu J, Handisides DR, Van Valckenborgh E, De Raeve H, Menu E, Vande Broek I, et al. Targeting the multiple myeloma hypoxic niche with TH-302, a hypoxia-activated prodrug. Blood 2010;116:1524–7.
34. Jeggo PA, Kemp LM. X-ray-sensitive mutants of Chinese hamster ovary cell line. Isolation and cross-sensitivity to other DNA-damaging agents. Mutat Res 1983;112:313–27.
35. Hoy CA, Thompson LH, Mooney CL, Salazar EP. Defective DNA cross-link removal in Chinese hamster cell mutants hypersensitive to bifunctional alkylating agents. Cancer Res 1985;45:1737–43.
36. Fuller LF, Painter RB. A Chinese hamster ovary cell line hypersensitive to ionizing radiation and deficient in repair replication. Mutat Res 1988;193:109–21.
37. Kuraoka I, Kobertz WR, Ariza RR, Biggerstaff M, Essigmann JM, Wood RD. Repair of an interstrand DNA cross-link initiated by ERCC1-XPF repair/recombination nuclease. J Biol Chem 2000;275:26632–6.
38. Liu N, Lamerdin JE, Tebbs RS, Schild D, Tucker JD, Shen MR, et al. XRCC2 and XRCC3, new human Rad51-family members, promote chromosome stability and protect against DNA cross-links and other damages. Mol Cell 1998;1:783–93.
39. Powell SN, Kachnic LA. Roles of BRCA1 and BRCA2 in homologous recombination, DNA replication fidelity and the cellular response to ionizing radiation. Oncogene 2003;22:5784–91.
40. Thompson LH, Hinz JM. Cellular and molecular consequences of defective Fanconi anemia proteins in replication-coupled DNA repair: mechanistic insights. Mutat Res 2009;668:54–72.
41. Gu Y, Patterson AV, Atwell GJ, Chernikova SB, Brown JM, Thompson LH, et al. Roles of DNA repair and reductase activity in the cytotoxicity of the hypoxia-activated dinitrobenzamide mustard PR-104A. Mol Cancer Ther 2009;8:1714–23.
42. Bindra RS, Schaffer PJ, Meng A, Woo J, Maseide K, Roth ME, et al. Down-regulation of Rad51 and decreased homologous recombination in hypoxic cancer cells. Mol Cell Biol 2004;24:8504–18.
43. Bindra RS, Gibson SL, Meng A, Westermark U, Jasin M, Pierce AJ, et al. Hypoxia-induced down-regulation of BRCA1 expression by E2Fs. Cancer Res 2005;65:11597–604.
44. Chan N, Koritzinsky M, Zhao H, Bindra R, Glazer PM, Powell S, et al. Chronic hypoxia decreases synthesis of homologous recombination proteins to offset chemoresistance and radioresistance. Cancer Res 2008;68:605–14.
45. Konstantinopoulos PA, Spentzos D, Karlan BY, Taniguchi T, Fountzilas E, Francoeur N, et al. Gene expression profile of BRCAness that correlates with responsiveness to chemotherapy and with outcome in patients with epithelial ovarian cancer. J Clin Oncol 2010;28:3555–61.
46. Singh S, Le H, Shih SJ, Ho B, Vaughan AT. Suberoylanilide hydroxyamic acid modification of chromatin architecture affects DNA break formation and repair. Int J Radiat Oncol Biol Phys 2010;76:566–73.
47. Yarde DN, Oliveira V, Mathews L, Wang X, Villagra A, Boulware D, et al. Targeting the Fanconi anemia/BRCA pathway circumvents drug resistance in multiple myeloma. Cancer Res 2009;69:9367–75.
48. Choudhury A, Zhao H, Jalali F, Al Rashid S, Ran J, Supiot S, et al. Targeting homologous recombination using imatinib results in enhanced tumor cell chemosensitivity and radiosensitivity. Mol Cancer Ther 2009;8:203–13.
49. Wachters FM, van Putten JW, Maring JG, Zdzienicka MZ, Groen HJ, Kampinga HH. Selective targeting of homologous DNA recombination repair by gemcitabine. Int J Radiat Oncol Biol Phys 2003;57:553–62.
50. Wouters BG, Brown JM. Cells at intermediate oxygen levels can be more important than the "hypoxic fraction" in determining tumor response to fractionated radiotherapy. Radiat Res 1997;147:541–50.

Downloaded from mct.aacrjournals.org on April 29, 2017. © 2011 American Association for Cancer Research.

Published OnlineFirst December 6, 2011; DOI: 10.1158/1535-7163.MCT-11-0634

AACR American Association for Cancer Research

Molecular Cancer Therapeutics

Molecular and Cellular Pharmacology of the Hypoxia-Activated Prodrug TH-302

Fanying Meng, James W. Evans, Deepthi Bhupathi, et al.

Mol Cancer Ther Published OnlineFirst December 6, 2011.

Updated version	Access the most recent version of this article at: doi:10.1158/1535-7163.MCT-11-0634
Supplementary Material	Access the most recent supplemental material at: http://mct.aacrjournals.org/content/suppl/2011/12/06/1535-7163.MCT-11-0634.DC1

E-mail alerts	Sign up to receive free email-alerts related to this article or journal.
Reprints and Subscriptions	To order reprints of this article or to subscribe to the journal, contact the AACR Publications Department at pubs@aacr.org.
Permissions	To request permission to re-use all or part of this article, contact the AACR Publications Department at permissions@aacr.org.

Downloaded from mct.aacrjournals.org on April 29, 2017. © 2011 American Association for Cancer Research.